

Received August 20, 2019; reviewed; accepted December 17, 2019

## Effect of grinding media on the flotation of copper-activated marmatite

Tao Long <sup>1</sup>, Yao Chen <sup>1</sup>, Juanjuan Shi <sup>1</sup>, Wei Chen <sup>1,2</sup>, Yangge Zhu <sup>2</sup>, Chonghui Zhang <sup>1</sup>, Xianzhong Bu <sup>1</sup>

<sup>1</sup> School of Resource Engineering, Xi'an University of Architecture and Technology, Xi'an, 710055, China

<sup>2</sup> State Key Laboratory of Mineral Processing, BGRIMM Technology Group, Beijing, China

Corresponding author: csuchenwei@csu.edu.cn (Wei Chen)

**Abstract:** How to avoid the shortage of floatability and non-purpose flotation in marmatite flotation is a big problem. This paper innovatively studies how to reduce these two negative phenomena from the perspective of grinding media. The effects of steel and stainless-steel balls on the flotation performance of copper-activated marmatite were investigated mainly through flotation tests, redox potential measurements, ion concentration tests, and XPS and FT-IR spectrum studies. The flotation results showed that the floatability of copper-activated marmatite remarkably decreased by using the steel ball in the grinding process, but it had a mere influence when stainless-steel medium was used. Redox potential measurements showed that the grinding environment of stainless-steel medium could exhibit a higher oxidizing potential than the steel grinding environment. Results from FTIR, XPS, and ion concentration measurements demonstrated that more ferric ions existed on the copper-activated marmatite surface in the steel grinding environment than that in the stainless-steel environment. Ferric ions could further hinder the activation effect of copper ions on marmatite and result in decreased marmatite flotation. This research could potentially explain the mechanism of ferric ions in the grinding process, and it can be utilized to improve the flotation performance of marmatite ore through selecting suitable grinding media in ball mill operations.

**Keywords:** grinding media, copper-activated marmatite, flotation separation, surface property

### 1. Introduction

In the mineral processing field, grinding is a complicated physicochemical process and has a significant impact on subsequent flotation processing. It has been recognized that the flotation behavior of sulfide ores is strongly influenced by the grinding environment (Yao et al., 2019). The grinding media could exhibit various effects on the flotation pulp, such as pH, redox potential, dissolved oxygen and ion concentration (Song et al., 2018). It has been found that porcelain grinding medium could reduce the galvanic interaction between porphyry copper and the corresponding grinding medium, ultimately improving the floatability of porphyry copper (Corin et al., 2018). It has also been demonstrated that the flotation separation of chalcopyrite, galena and gold from pyrite are also deeply affected by the grinding media used in the size-reduction process (Mu et al., 2018). When stainless steel and low carbon steel media are adopted in the re-grinding-flotation process, it has also been proven that the flotation of pyrite in the subsequent scavenging stage is also different (Chen et al., 2013).

Marmatite is a typical sulfide mineral of zinc and usually associated with chalcopyrite, porphyry copper in ore deposits. Copper-containing minerals have been found to easily dissolve and release copper ions in the grinding process, which could further result in the activation of marmatite and separation problems in the subsequent flotation operations (Pearse, 2005; Xiao et al., 2019). In the pyrite flotation, it has been found that the grinding medium has a certain effect on the flotation of Cu<sup>2+</sup> activated pyrite (Owusu et al., 2014). Therefore, there is a large possibility that the grinding medium

would also exhibit some effects on the copper-activated marmatite that may constitute the main cause of the above mentioned separation problem (Huang et al., 2020; Zhenguo et al., 2017). It is very important to clarify the specific influence of the grinding medium on the marmatite flotation (Liu et al., 2013). However, to date, there are no published reports on  $\text{Cu}^{2+}$  activated marmatite flotation related to the grinding medium selection.

It has been shown that marmatite has good floatability under alkaline conditions (around pulp pH 10-11) (Xiao et al., 2014). Research on activation of marmatite using copper ions revealed that  $\text{Cu}_n\text{S}$  might exist on the surface of  $\text{Cu}^{2+}$ -activated marmatite (Rashid et al., 2019). As the redox potential changes, the index  $n$  could vary between 1 and 2. It has been found that  $\text{CuS}$  dominates the marmatite surface under high redox potential, and  $\text{Cu}_2\text{S}$  will cover most of the marmatite surface if the redox potential is relatively low. In this circumstance, it is very likely that the activation effect of the copper ions could be enhanced by decreasing the redox potential (Chandra and Gerson, 2009).

The objective of this study is to reveal the effect of the grinding medium on the flotation behaviors of copper ion activated marmatite. Two grinding media, steel and stainless-steel balls, were used. The surface properties of marmatite under different grinding mediums were analyzed by flotation test, potential measurement, ion concentration tests, XPS and FT-IR spectra studies.

## 2. Materials and methods

### 2.1. Materials and reagents

The marmatite sample was obtained from Xitieshan Mine, Qinghai province, China. A large chunk of marmatite crystal was crushed through a jaw crusher. The pure marmatite crystal was hand-picked, further crushed in a roll crusher and dry-sieved. The 0.5~3.2 mm fractions were stored for subsequent grinding, flotation, zeta potential, and XPS measurements. The purity of the mineral sample was 96.37%, according to its X-ray diffraction results and chemical analysis, which can be found in our previous research paper (Bu et al., 2019).

Butyl xanthate (BX) and pine oil, which used as collector and frother respectively in this research, were purchased from Zhuzhou Flotation Reagents Factory, Hunan, China. They were used as the collector and frother, respectively. Copper nitrate ( $\text{Cu}(\text{NO}_3)_2 \cdot 3\text{H}_2\text{O}$ ) and polymerization ferric chloride (PFC) ( $\text{FeCl}_3$ ) were bought from Tianjing Kermil Chemical Reagents Development Centre, Tianjin, China. Sodium hydroxide (NaOH) was used as a pH regulator. All reagents were analytically pure. Deionized water (conductivity =18.2  $\text{M}\Omega \text{ cm}$ ) was used for all tests.

### 2.2. Grinding tests

The crushed mineral samples, -3.2+0.5 mm fractions, were respectively ground by steel (see Fig. 1a) and stainless-steel balls (see Fig. 1b) in a RK/ZQM type 150×50 mill (Wuhan Rock Mill Equipment Manufacturing Co., Ltd).

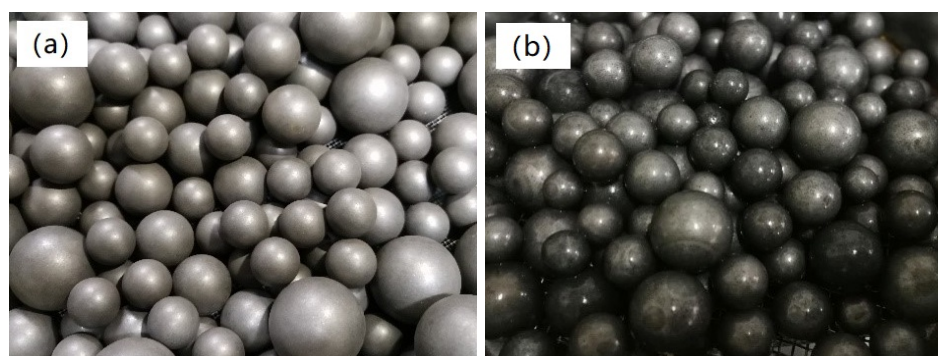


Fig. 1. The steel (a) and stainless-steel (b) balls used in this study

The filling rate of the both grinding media was controlled at 40%. The volume ratio of the grinding environment was set as big ball: middle ball: small ball = 4:3:3 (big ball:  $\Phi 25\text{mm}$ ; middle ball:  $\Phi 18 \text{ mm}$ ; small ball:  $\Phi 14 \text{ mm}$ ). For each grinding test, 40 g of marmatite and 60 mL of  $\text{Cu}(\text{NO}_3)_2 \cdot 3\text{H}_2\text{O}$  solution

( $3.8 \times 10^{-3}$  mol/L) was fed into the mill and ground for 5 min. After grinding, the products were sieved using a standard screen with a pore size of 74  $\mu\text{m}$ . Particles coarser than 74  $\mu\text{m}$  were returned to the mill for re-grinding where the particles finer than 74  $\mu\text{m}$  were sieved again using a 38  $\mu\text{m}$  screen to obtain size fractions between 38 and 74  $\mu\text{m}$ . Samples were then rinsed with deionized water and used for flotation tests.

### 2.3. Flotation tests

Flotation tests were carried out in a 0.5 L RK/FD (Wuhan Rock Mill Equipment Manufacturing Co., Ltd) flotation machine at an impeller speed of 1500 rpm. The mineral suspension was prepared by adding 40 g of mineral sample and 450 mL of deionized water into the flotation cell and agitated for 2 min. Pulp pH was adjusted by adding corresponding pH regulators. BX was added at a desired concentration and conditioned for 3 min. Pine oil was added at a 20 mg/L concentration and conditioned for 0.5 min before flotation. Flotation lasted for 3 min. After flotation, the products were collected, filtered, dried and weighted. Flotation recovery was directly calculated by the weight distribution of dry flotation products.

In this research, each grinding and subsequent flotation test was repeated at least 3 times and the mean value was taken as the final flotation data. The standard deviation was calculated and presented as error bars.

### 2.4. Redox potential (Eh) and pH measurements

In order to detect the dynamic changes of redox potential (Eh) and pH in the subtle grinding/flotation process, a HI991002 portable pH/ORP/temperature tester (Hanna Instruments, Italy) was used to measure redox potentials: after grinding, after conditioning, after adding BX, after adding pine oil and after aeration. The probe of the tester was immersed into the mineral slurry and the potential value was recorded on line.

### 2.5. Ion concentration measurements

In this study, the  $\text{Cu}^{2+}$  concentration in the slurry filtrate was detected with an inductively coupled plasma mass spectrometry-Thermo X Series II (ICP-MS) (Thermo Scientific Instruments, China). After stabilizing the plasma for at least 30 min, the  $\text{Cu}^{2+}$  concentration was recorded. In this study, each measurement was repeated at least three times and the average results were chosen and presented.

### 2.6. X-ray photoelectron spectroscopy measurements

In this research, an ESCAALAB 250Xi (Thermo Scientific Co, China) with aluminum anode was used to obtain the X-ray photoelectron spectroscopy of the mineral samples with specified surface treatments. The X-ray source was Al K $\alpha$  radiation (1486.71eV) at a pressure of  $1 \times 10^{-6}$  Pa in the analytical chamber. All binding energies were referenced to the natural C1s peak at 284.5 eV to compensate for surface charging effects. The samples were firstly scanned in a survey mode to determine the concentrations of elements on the surfaces of the particles, and then information on the chemical bonds and oxidation states of the elements was obtained in high-resolution mode. The spectra were processed using Casa XPS software.

### 2.7. Infrared spectra tests

In this research, the infrared spectra of mineral samples treated with flotation reagents were recorded with an FT-IR Fourier Transform Infrared Spectrometer (Nicolet instrument company, Japan) by the KBr diffuse reflection method. For each measurement, 1.0 g of pure mineral (about 2  $\mu\text{m}$  in size) was ultrasonically dispersed in 20 mL deionized water. Then, the flotation reagents were added in sequence to a desired concentration ( $c(\text{Cu}^{2+}) = 3.8 \times 10^{-3}$  mol/L,  $c(\text{FeCl}_3) = 2 \times 10^{-4}$  mol/L). The pulp was conditioned with a magnetic stirrer at 25°C and pH 10, and the conditioning time for each reagent was 40 min. After conditioning, the suspensions were centrifuged. The precipitation was washed 3 times with deionized water and then dried at 40 °C in a vacuum oven. Lastly, the dry mineral samples were

collected for infrared detection at room temperature. The wave number range of the spectra was 400 – 4000  $\text{cm}^{-1}$ . Each spectrum was recorded with 30 scans measured at 2  $\text{cm}^{-1}$  resolution.

### 3. Results and discussion

#### 3.1. Flotation experiment results

Different flotation behaviors of marmatite products were obtained by different grinding media under an increasing BX concentration in the presence and absence of  $\text{Cu}^{2+}$ . Flotation tests on the marmatite samples that were obtained using both grinding environments ( $c(\text{Cu}^{2+}) = 3.8 \times 10^{-3} \text{ mol/L}$ ,  $\text{pH} = 10$ ) in the presence and absence of  $\text{Cu}^{2+}$  were conducted under an increasing BX collector dosage, and the results are shown in Fig. 2.

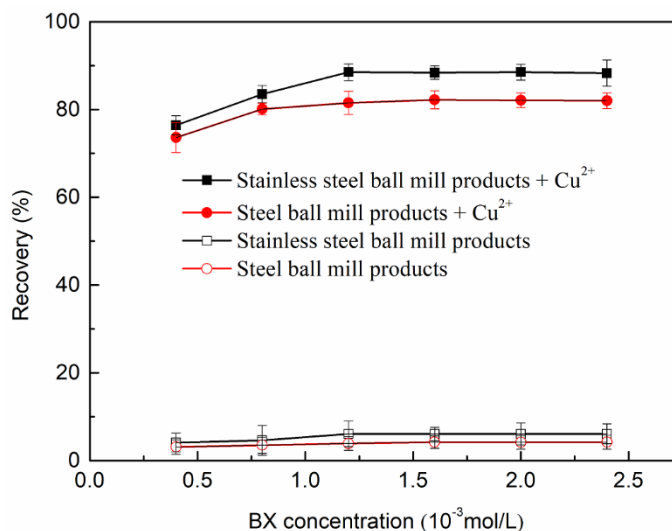


Fig. 2. The flotation recovery of marmatite as a function of BX dosage in the absence and presence of copper ion acting as activator

It can be seen that marmatite exhibited poor floatability in the absence of  $\text{Cu}^{2+}$  activator. The marmatite flotation recovery remained low (less than 10%) across the whole BX concentration tested. When  $\text{Cu}^{2+}$  was introduced, flotation recovery of the marmatite significantly increases (more than 70%). This large improvement in marmatite floatability was attributed to the activation effect of  $\text{Cu}^{2+}$  on the marmatite particles. Meanwhile, the flotation performances of marmatite ground by the two grinding media were different. The flotation recovery of the stainless-steel ball mill products was always higher than that of the steel ball mill products in the BX concentration investigated. The activation effect of  $\text{Cu}^{2+}$  could be influenced by the type of grinding medium, and the steel ball grinding medium could negatively affect marmatite flotation.

#### 3.2. Eh measurement results

Eh levels of the different grinding products are indicated in Table 1. The Eh value of pulp after grinding was greater than that of the stainless-steel medium (in Table 1).

Table 1. shows the change of redox potential (Eh) in the grinding-flotation stage. After grinding, the Eh potential of the stainless-steel medium was 54 mV higher than that of the steel ball medium, which indicated that the Eh potential in the steel ball medium was lower and the system exhibited stronger reducibility (Mu and Peng, 2019). Because the more reductive steel ball medium interacts with minerals in the grinding process, the redox potential of the minerals is reduced (Rabieh et al., 2016). With the flotation test, the potential difference between the two-grinding media reduced. After the addition of BX, xanthic acid produced by the hydrolysis of BX, caused gradual decrease in the redox potential. The low-potential reducing environment caused by grinding of the iron medium was not conducive to the oxidation of BX into dixanthogen, while the high-potential oxidizing environment caused by grinding of the chemical inert (such as ceramic ball) medium could contribute to the oxidation of BX into

dixanthogen (Xiao et al., 2014). This may be one of the reasons for the difference in floatability between the two-grinding media (Nie et al., 2019).

Table 1. The pulp Eh value in different stages using different grinding media

Grinding medium	Eh(mV)				
	After grinding	Conditioning	BX	After pine oil	Aeration
Stainless Steel	-74	-28	-144	-141	-129
Steel ball	-128	-42	-148	-145	-139

### 3.3. Ion concentration measurement results

An ICP analysis was used to detect the influence of different grinding media on  $\text{Cu}^{2+}$  content in slurry filtrate of marmatite.

Table 2. Influence of grinding media on  $\text{Cu}^{2+}$  content

Grinding medium	Added $\text{Cu}^{2+}$ ( $10^{-3}$ mol/L)	Residual $\text{Cu}^{2+}$ in filtrate ( $10^{-6}$ mol/L)	Flotation recovery (%)
Steel ball	3.8	0.4	78.6
Stainless ball	3.8	0.9	83.5

The concentration of  $\text{Cu}^{2+}$  in the steel ball medium was  $0.5 \times 10^{-6}$  mol/L less than that in the filtrate of the stainless-steel medium (see Table 2). Therefore, compared to the steel ball medium, the stainless-steel medium was not helpful to the adsorption of copper ions on the surface of marmatite. Marmatite surface can adsorb more copper ions in the steel ball medium than in the stainless steel-medium. Copper ions can promote the flotation of marmatite (Chen and Yoon, 2000), but the flotation test results show that the recovery of marmatite in the stainless-steel medium was 4.9% higher than that in the steel ball medium. This indicates that there are interactions in the steel ball medium that could hinder the activation process of marmatite by copper ions, and thus results in poor floatability. In the stainless-steel medium, the interaction could promote the activation of copper ions on marmatite.

### 3.4. XPS measurement results

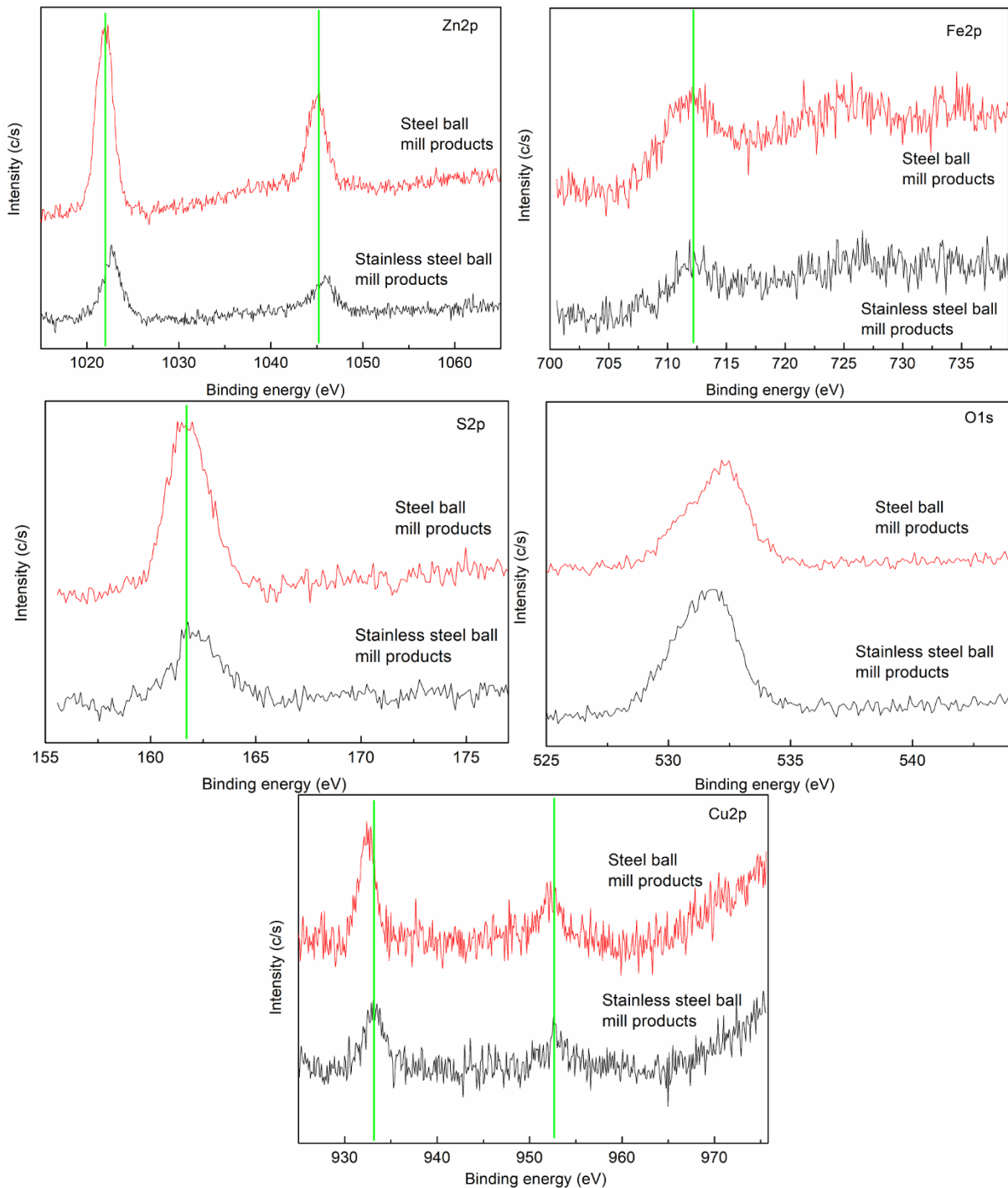
The changes of atomic concentration on the surface of marmatite in different grinding media were measured and the results are shown in Table 3 and Fig 3.

Table 3. Marmatite surface atomic concentration (%)

Grinding medium	Atomic concentration (%)				
	O1s	S2p	Cu2p	Zn2p	Fe2p
Steel ball	14.74	9.15	0.10	4.91	0.34
Stainless ball	11.88	4.45	0.01	1.99	0.24

Table 3 shows that the surface composition of  $\text{Cu}^{2+}$ -activated marmatite was affected by different grinding media, and all atomic concentrations in the stainless-steel medium were lower than those in the steel ball medium. In the stainless-steel medium, the concentration of copper atoms and iron atoms on the surface of marmatite decreased significantly. The surface of marmatite contained more Fe and Cu, indicating that in the steel ball medium, more hydroxide and oxide of hydrophilic iron on the surface of marmatite were adsorbed than the stainless-steel medium (Jia et al., 2000; Xiao et al., 2018).

In the steel ball medium, the ratios of Zn:S and Fe:S were 1:2.18 and 1:26.91, respectively, while in the stainless-steel medium the ratios were Zn:S 1:2.24 and Fe:S=1:18.54, respectively. Marmatite formed a sulfur-rich and metal-deficient surface under both media.



**Fig. 3.** The xps spectrograms of the relative elements in marmatite samples treated with different grinding media

It can be concluded from Fig. 3 that in the case of grinding using the steel ball medium, the binding energy of 711.4 eV in Fig. 3(Fe2p) corresponded to  $\text{Fe}^{3+}$  in  $\text{FeOOH}$ , and the binding energy of 713.92 eV was iron hydroxide. In Fig. 3(S2p), the binding energy of 162.04 eV corresponded to  $\text{FeS}_2$ . In Fig. 3(Cu2p), the binding energy of 932.31 eV corresponded to  $\text{CuS}$  and the binding energy of 932.9 eV was  $\text{Cu}_2\text{S}$ . This indicates that iron hydroxide,  $\text{FeOOH}$ ,  $\text{FeS}_2$ ,  $\text{CuS}$ ,  $\text{Cu}_2\text{S}$  and other substances were generated on the surface of marmatite. In the case of grinding using the stainless-steel medium, the binding energy of 710.7 eV in Fig. (b) corresponded to  $\text{Fe}_2\text{O}_3$ . In Fig. 3(S2p),  $\text{FeS}_2$  could correspond to the binding energy

of 162.16 eV and  $S^0$  could correspond to the binding energy of 164.01 eV. In Fig. 3(Cu2p), the binding energy of 934.6 eV corresponded to  $Cu(OH)_2$ . This indicates that  $Fe_2O_3$ ,  $FeS_2$ ,  $Cu(OH)_2$ ,  $S^0$  and other substances were generated on the surface of marmatite.

To sum up, in the steel ball medium, after the ion exchange between Zn and Cu on the surface of marmatite, parts of  $Cu^{2+}$  were reduced to  $Cu^+$ , and  $Cu^+$  reacted with sulfur to form  $Cu_2S$ . Because of the electrostatic adsorption between  $Fe(OH)_3$  and marmatite activated by  $Cu^{2+}$  (Bokanyi et al., 2016), a large amount of  $Fe(OH)_3$  could cover the surface of marmatite and hinder the capture of marmatite by the collector BX. In stainless steel medium,  $Cu(OH)_2$  and hydrophobic  $S^0$  were largely formed on the surface of marmatite, which improved the floatability of marmatite.

### 3.5. Infrared spectroscopic results

XPS analysis shows that the stainless steel medium, compared to the steel ball medium, more easily produced a large amount of iron hydroxide. In order to further prove the existence of a large number of iron ions on the surface of marmatite, an infrared spectral analysis was used to study the influence of iron ions on the surface of marmatite, as well as the effect of iron ions on the adsorption characteristics of BX on the surface of marmatite. The test results are shown in Fig. 4.

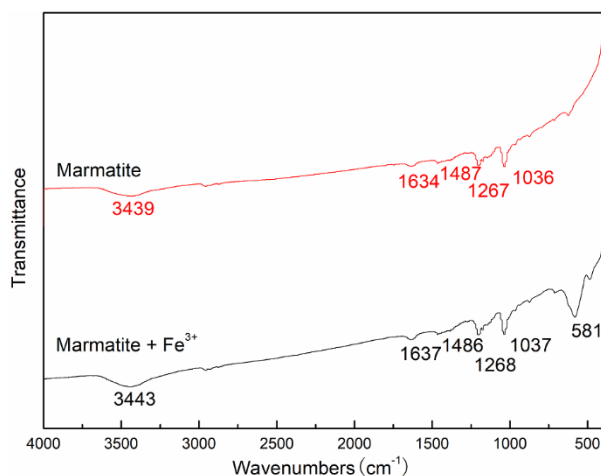


Fig. 4. Infrared spectrum of the marmatite samples (with BX pretreatment) with  $Fe^{3+}$  treatment

As shown in Fig. 4, 1037 and 1036  $cm^{-1}$  peaks were corresponded to the BX adsorption. Peaks at 1268 and 1267  $cm^{-1}$  exhibited a notable adsorption and was the characteristic band for the dixanthogen C-O-C bond. In addition, 1487 and 1486  $cm^{-1}$  were adsorption peaks of xanthogenate  $CSS^-$  (Yu and Qiu, 2004). The characteristic adsorption peak of dixanthogen was significantly higher than that of  $CSS^-$  xanthate, indicating that, after the interaction of xanthate and marmatite, the products on the surface of marmatite were mainly dixanthogen, accompanied by a small amount of xanthate. Peaks at 3443, 3439, 1637 and 1634  $cm^{-1}$  were the results of the  $OH^-$  adsorption. After adding  $Fe^{3+}$ , the adsorption peak intensity of BX increased slightly, suggesting that  $Fe^{3+}$  had little effect on the adsorption of xanthate. However, the  $OH^-$  adsorption peak intensity of marmatite +  $Fe^{3+}$  (black line) was significantly greater than marmatite (red line) (in Fig. 4). Marmatite surface generated a large amount of hydrophilic ferric hydroxide, which led to the mineral surface being hydrophilic. This does not contribute to the marmatite flotation. The results further proved that the existence of  $Fe^{3+}$  can lead to the production of ferric hydroxide on the surface of marmatite.

## 4. Conclusions

The following conclusions can be drawn from this study:

- (1) Bare marmatite could exhibit electrostatic repulsion with ferric hydroxide, which prevents iron hydroxide from adsorbing on the surface of marmatite. Copper ion activated marmatite and ferric hydroxide have electrostatic attraction interactions, which could hinder the collector adsorption on its surface.

- (2) After grinding, the slurry potential of the stainless-steel ball medium was 54 mV higher than that of the steel ball medium, indicating that the steel ball medium produced more hydrophilic iron hydroxide that adsorbed on the surface of marmatite. The stainless steel ball medium was more beneficial for the copper activated marmatite flotation, for its high-potential oxidizing environment could promote the generation of trace  $\text{Cu}(\text{OH})_2$  and hydrophobic  $\text{S}^0$ .
- (3) The low potential reducing environment caused by steel ball grinding is not helpful to the oxidation of xanthate, while the high potential oxidizing environment could contribute to the oxidation of xanthate.

### Acknowledgments

The work was funded by National Natural Science Foundation of China (Grant No. 51904221), the Open Foundation of State Key Laboratory of Mineral Processing (Grant No. BGRIMM-KJSKL-2020-05), the Project funded by China Postdoctoral Science Foundation (Grant No. 2018M640964 and 2019T120884), the General Project (Youth) of Natural Science Basic Research funded by Shaanxi Science and Technology Department (Grant No. 2019JQ-368 and 2019JQ-545), and the Natural Science Project of Shaanxi Education Department (Grant No. 19JK0465), and the RenCai Technology Fund of Xi'an University of Architecture and Technology (Grant No. RC1820).

### References

- BU, X., CHEN, F., CHEN, W., DING, Y., 2019. *The effect of whey protein on the surface property of the copper-activated marmatite in xanthate flotation system*. Applied Surface Science 479, 303-310.
- BOKÁNYI, L., SZABÓ, S., PAULOVICS, J., 2016. *Investigation of surface properties and floatability of CDTE semiconductor for the sake of recycling of obsolete solar elements*. Can. Inst. Mining, Metall. Pet. IMPC 2016, p. 9.
- CHANDRA, A.P., GERSON, A.R., 2009. *A review of the fundamental studies of the copper activation mechanisms for selective flotation of the sulfide minerals, sphalerite and pyrite*. Advances in colloid and interface science 145, 97-110.
- CHEN, X., PENG, Y., BRADSHAW, D., 2013. *Effect of regrinding conditions on pyrite flotation in the presence of copper ions*. International Journal of Mineral Processing 125, 129-136.
- CHEN, Z., YOON, R.H., 2000. *Electrochemistry of copper activation of sphalerite at pH 9.2*. International Journal of Mineral Processing 58, 57-66.
- CORIN, K.C., SONG, Z.G., WIESE, J.G., O'CONNOR, C.T., 2018. *Effect of using different grinding media on the flotation of a base metal sulphide ore*. Minerals Engineering 126, 24-27.
- HUANG, X., ZHU, T., DUAN, W., LIANG, S., LI, G., XIAO, W., 2020. *Comparative studies on catalytic mechanisms for natural chalcopyrite-induced Fenton oxidation: Effect of chalcopyrite type*. Journal of Hazardous Materials 381, 120998.
- JIA, J., XIE, X., WU, D., WANG, J., WANG, Y., 2000. *An XPS Study on Surfaces of Common Sulfide Minerals*. Geological Journal of China Universities 6, 255-259.
- LIU, W., MORAN, C.J., VINK, S., 2013. *A review of the effect of water quality on flotation*. Minerals Engineering 53, 91-100.
- MU, Y., PENG, Y., 2019. *The effect of saline water on copper activation of pyrite in chalcopyrite flotation*. Minerals Engineering 131, 336-341.
- MU, Y., PENG, Y., LAUTEN, R.A., 2018. *The galvanic interaction between chalcopyrite and pyrite in the presence of I lignosulfonate-based biopolymers and its effects on flotation performance*. Minerals Engineering 122, 91-98.
- NIE, X., FENG, S., ZHANG, S., GAN, Q., 2019. *Simulation study on the dynamic ventilation control of single head roadway in high-altitude mine based on thermal comfort*. Advances in Civil Engineering 2019, 12.
- OWUSU, C., FORNASIERO, D., ADDAI-MENSAH, J., ZANIN, M., 2014. *Effect of regrinding and pulp aeration on the flotation of chalcopyrite in chalcopyrite/pyrite mixtures*. Powder Technology 267, 61-67.
- PEARSE, M.J., 2005. *An overview of the use of chemical reagents in mineral processing*. Minerals Engineering 18, 139-149.
- RABIEH, A., ALBIJANIC, B., EKSTEEN, J.J., 2016. *A review of the effects of grinding media and chemical conditions on the flotation of pyrite in refractory gold operations*. Minerals Engineering 94, 21-28.
- RASHID, M.I., BENHELAL, E., FARHANG, F., OLIVER, T.K., RAYSON, M.S., BRENT, G.F., STOCKENHUBER, M., KENNEDY, E.M., 2019. *Development of Concurrent grinding for application in aqueous mineral carbonation*. Journal of Cleaner Production 212, 151-161.
- SONG, Z.G., CORIN, K.C., WIESE, J.G., O'CONNOR, C.T., 2018. *Effect of different grinding media composition on the*

- flotation of a PGM ore. Minerals Engineering 124, 74-76.*
- SONG, Z.G., CORIN, K.C., WIESE, J.G., O'CONNOR, C.T., 2017. *Effect of Grinding Medium Type and Collector Addition Site on Flotation of a Cu-Ni Sulphide Ore. Conservation and Utilization of Mineral Resources 6, 36-40.*
- XIAO, Q., BO, L., KANG, H., 2014. *The Effect of Fine Grinding Medium Feature on Grinding Results. Aasri Procedia 7, 120-125.*
- XIAO, W., REN, Y., YANG, J., CAO, P., WANG, J., QIN, W., QIU, G., 2019. *Adsorption mechanism of sodium oleate and styryl phosphonic acid on rutile and amphibole surfaces. Transactions of Nonferrous Metals Society of China 29, 1939-1947.*
- XIAO, W., ZHAO, Y., YANG, J., REN, Y., YANG, W., HUANG, X., ZHANG, L., 2019. *Effect of Sodium Oleate on the Adsorption Morphology and Mechanism of Nanobubbles on the Mica Surface. Langmuir 35, 9239-9245.*
- YAO, W., LI, M., ZHANG, M., CUI, R., JIANG, H., LI, Y., ZHOU, S., 2019. *Effects of grinding media on flotation performance of calcite. Minerals Engineering 132, 92-94.*
- YU, R., QIU, G., HU, Y., QIN, W., 2004. *Adsorption Mechanism of Ethyl Xanthate on Marmatite. Metal Mine 342, 29-31.*
- ZHANG, C., LI, L., YUAN, Z., XU, X., SONG, Z., ZHANG, Y.R., 2020. *Mechanical properties of siderite and hematite from DFT calculation. Minerals Engineering 146, 106107.*